



Mechanical Properties of HVOF Coatings

O.C. Brandt

High-velocity oxygen fuel (HVOF) thermal-sprayed carbide coatings are distinguished by high hardness, low porosity, and good wear resistance compared to other thermal spray technologies. However, for many engineering applications the ductility and fatigue resistance are the most important material properties. In the use of HVOF systems, these properties are influenced by many boundary conditions. This paper presents the effects of different spraying parameters on the fatigue resistance of samples coated by the HVOF process.

1. Introduction

HIGH-VELOCITY oxygen fuel (HVOF) thermal spraying is the newest variant in thermal spray technologies. Coatings produced by the HVOF process exhibit the following advantages (Ref 1):

- The high particle velocity renders a dense coating with a porosity level below 1% and a high bond strength of more than 80 MPa.
- The coatings have a low surface roughness.
- The thermally induced changes in the coating material are low in comparison to plasma spraying.

Thermal spray coatings are commonly used to lessen wear and corrosion and to rebuild surfaces. Their durability is mostly limited by corrosion or wear. Thermal spraying of machine parts must also consider service requirements, such as stresses imposed due to fatigue. It is known that the maximum fatigue limit of thermal sprayed parts is affected by grit blasting before the spray process. D-Gun™ (Praxair Surface Technologies, Inc., Danbury, CT, USA) sprayed tungsten carbide coatings have exhibited favorable fatigue resistance properties (Ref 2, 3). Knowledge of mechanical strength also is important for the use of HVOF coatings, especially in lightweight constructions.

2. Preliminary Theory

Coatings produced by the HVOF process are influenced by parameters that can be divided into primary and secondary categories, as shown in Fig. 1. Several mechanical properties contribute to the fatigue life of a material and are detailed below. The primary parameters involve the equipment, and the secondary involve the surface and shape of the part.

2.1 Elasticity

Hardness and density often are the major quality criteria for evaluating coatings. When evaluating the effect of mechanical

Keywords: Fatigue life, high-velocity oxygen fuel, parameterization, residual stress, spray process, substrate dependence, surface roughness, WC-Co feedstock

O.C. Brandt, Federal Armed Forces University at Hamburg, Institute for Machine Parts and Handling Technology, Holstenhofweg 85 D22039, Germany

strain, the Young's modulus of elasticity, E , is also an important design value. Applied forces may induce stress between the substrate and the coating because of their different E values, thus nucleating cracks under cyclic stress.

If HVOF carbide coatings are sprayed with a density below 1% of theoretical, the E moduli are nearly 40% of the value of sintered hard metals. The dependence of the E modulus on composition is shown in Fig. 2; measurements were made in a three-point bending test on aluminum and steel substrates.

Variations in spray parameters within typical ranges or different feedstock particle sizes showed no influence on the value of E . Young's modulus increases by 5% if nickel is used as the matrix material; if a cobalt-chrome matrix is used, the E decreases by 5%. The measured value is 90 GPa for a Cr_3C_2 -25NiCr coating and 132 GPa for a Cr_3C_2 -17Ni coating.

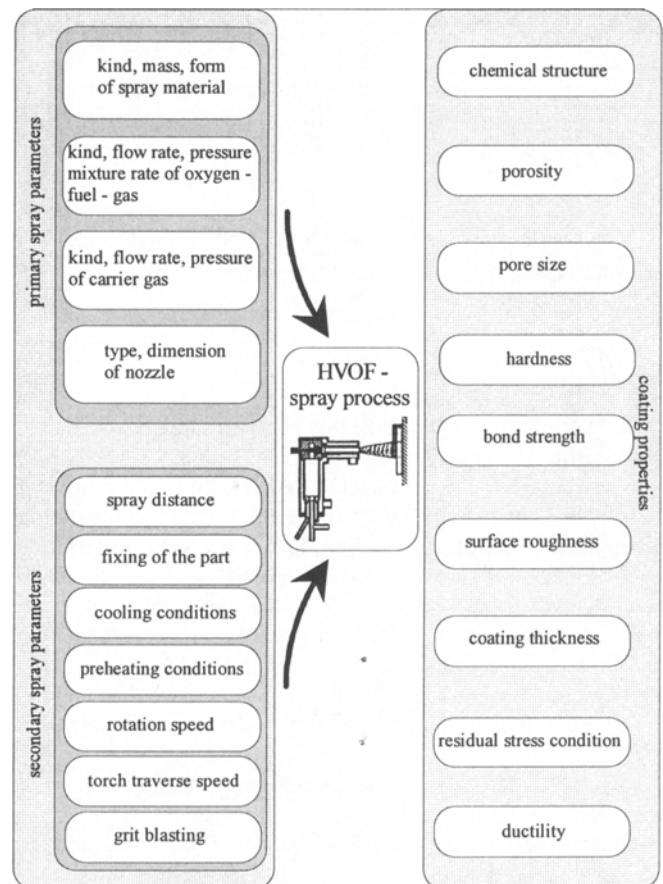


Fig. 1 Primary and secondary parameters in HVOF processes

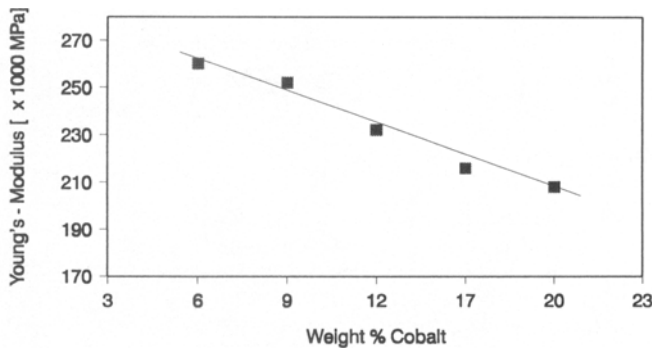


Fig. 2 Young's modulus of HVOF-sprayed tungsten carbide coatings as a function of cobalt concentration (20 tests on each coating)

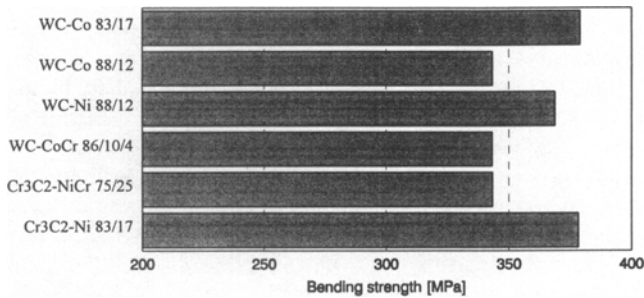


Fig. 3 Maximum bending strength of HVOF-sprayed carbide coatings

2.2 Strength

Maximum tensile strength is another important consideration in engineering design. The maximum tensile strength of HVOF tungsten carbide coatings was measured in a three-point bending test on aluminum substrates. Results are shown in Fig. 3.

The maximum value is influenced by the residual stress conditions caused by dissimilar metal coatings. These values may change for different surface shapes.

2.3 Residual Stress

A determining factor for the mechanical integrity of machine parts is often the unfavorable residual stress condition. Residual stress in sprayed parts arises from the difference in modulus of thermal expansion between the substrate and the coating during the cooldown phase after spraying. The direction (\pm) and the size (value) of these stresses are also influenced by the absolute temperature and the thickness relation of the substrate and the coating. Figure 4 illustrates the principle of residual stress formation in thermal sprayed coatings. It is evident that different residual stress conditions could exist in the same coatings when applied under same spray parameters but onto parts of different geometries.

The deformation f in Fig. 4 can be used to calculate the residual stress in a flat sample (Ref 4). For example, Fig. 5 shows the measured residual stress in an HVOF WC-17Co coating sprayed on a 5 mm thick aluminum substrate. The testing conditions used to generate these data are shown in Fig. 6. The coating thickness was varied by the number of spray paths. Variations in

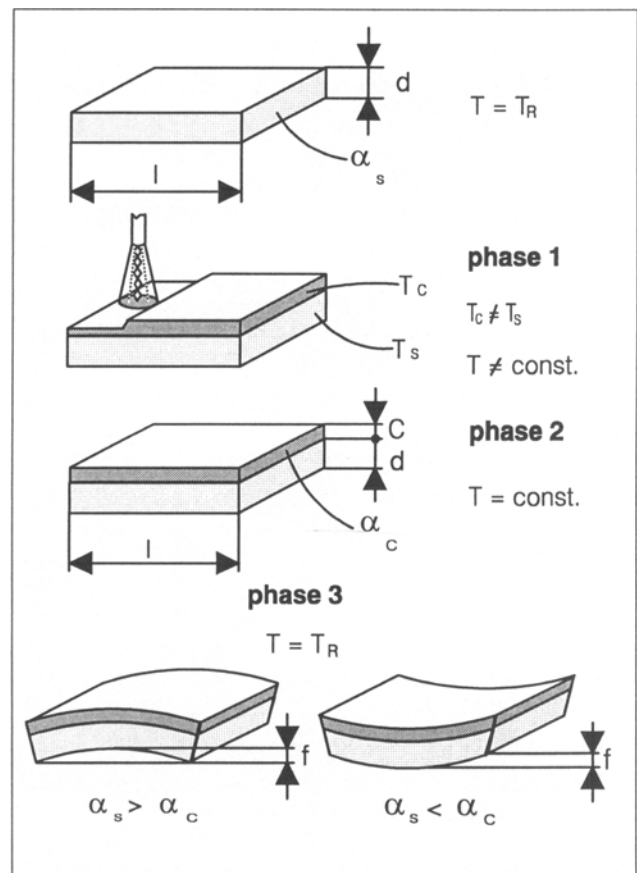


Fig. 4 Residual stress formation due to thermal spray processes. T , temperature; T_R , room temperature; T_C , coating temperature; T_S , substrate temperature; α_C , modulus of thermal expansion of coating material; α_S , modulus of thermal expansion of substrate material; l , sample length; d , sample thickness; c , coating thickness; f , deformation

the standoff distance between nozzle and substrate, torch traversing speed, rotation speed, powder feed rate, gas flow, and cooling rate may all influence residual stress.

3. Experimental Investigation

Under cyclic stress, residual stress is an important factor in determining maximum strain. To study the relation between spray parameters and cyclic strength, the same test conditions must be used for all test samples.

3.1 Methodology

Reference tests were sprayed with a Jet-Kote II™ (Deloro Stellite, Inc., Belleville, Ontario, Canada/Thermadyne Industries, Inc., St. Louis, MO, USA) system as depicted in Fig. 6. Typical parameters for spraying carbide coatings are given in Table 1.

Cyclic fatigue diagrams were obtained in a fatigue bending test using 12 samples with a 0.2 mm thick coating on both sides. To minimize scattering, all 12 samples were sprayed on the same section with constant dimensions. This allowed constant values of residual stress to be obtained, so that additional measurements of this property were unnecessary.

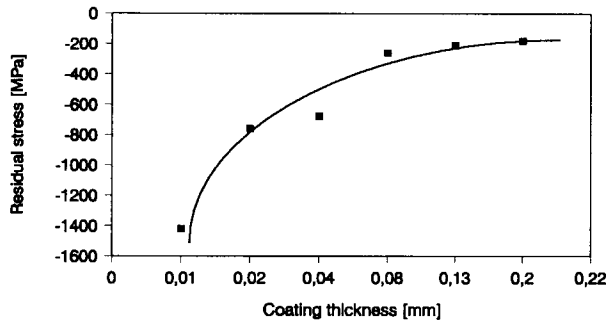


Fig. 5 Residual stress in 5 mm thick aluminum samples

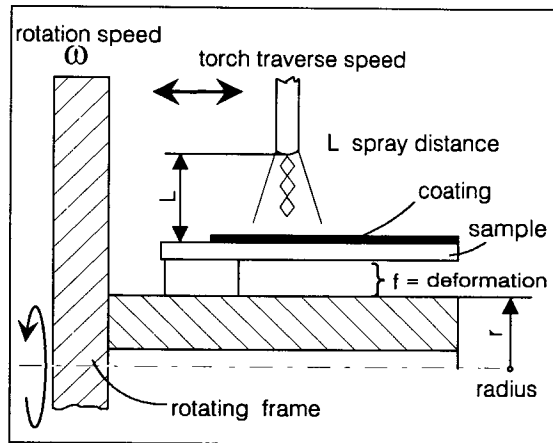


Fig. 6 Test conditions for coating preparation and measurement of residual stress

Table 1 Baseline parameters and typical ranges for spraying carbide coatings

Gun	Jet Kote II
Fuel gas	C ₃ H ₈
Fuel flow, L/min	40-60
Oxygen flow, L/min	350-420
Carrier gas	N ₂
Carrier flow, L/min	20-30
Powder feed rate, g/min	25-40
Gun/part surface speed, m/min	40-100
Torch forward speed, mm/rev	4-6
Spray distance, mm	200-300

Table 2 Mechanical properties of substrate materials

Material	Tensile strength, MPa	Yield strength, MPa	Breaking elongation, %	Hardness, HB
AlMg 3	220-260	165	9	65
St 37II	340-470	235	26	105

These measurements assume that residual stress is a function of the coating alloy and not of shape or geometry, which are held constant. Substrates included an aluminum alloy (AlMg 3) and a construction steel (St 37). The mechanical properties of the substrate materials are given in Table 2. To simplify comparison between the different coating materials and spray parameters,

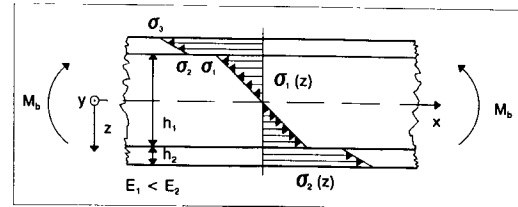


Fig. 7 Bending stress in an HVOF carbide coating. h_1 , substrate thickness; h_2 , coating thickness; E_1 , Young's modulus of substrate; E_2 , Young's modulus of coating; M_b , bending force; $\sigma_1(z)$, bending stress distribution of substrate; $\sigma_2(z)$, bending stress distribution of coating; σ_1 , maximum bending stress of substrate; σ_2 , maximum bending stress of coating; σ_3 , maximum bending stress of coating

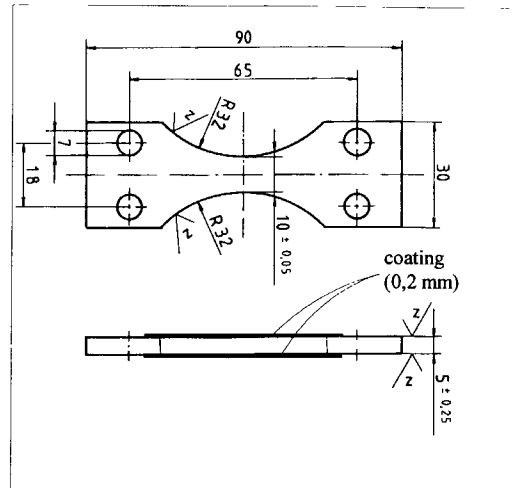


Fig. 8 Design of test samples. All dimensions in millimeters

the bending stress was calculated for a sample that was completely coated. This calculation considers the coating to be a component of the structure. The bending stress in an HVOF carbide coating is shown schematically in Fig. 7.

3.2 Fatigue Tests

The primary objective of this research was to clarify the basic relation between spray parameters and fatigue strength in order to optimize the fatigue resistance of the substrate material. Under cyclic stress, residual stress is an important factor in determining maximum strain. Proper study of the relation between spray parameters and cyclic strength requires the same test conditions for all test samples.

With regard to the dependence of residual stress on part shape, spray parameters can be compared only when those parameters have been obtained from experiments with constant boundary conditions. Therefore, only one parameter was varied in each experiment.

Exact determination of fatigue strength requires a large number of samples, generally at least 40 (Ref 5). The first runs showed no significant differences in the deviation of the maximum number of cycles at the same stress between HVOF-coated parts and the raw material. With respect to this result, 12 meas-

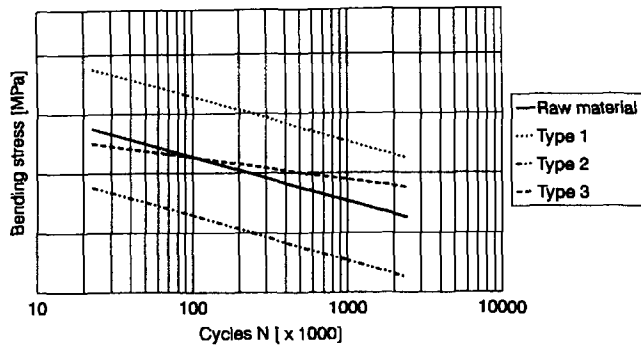


Fig. 9 Schematic illustrating three types of *S/N* curves

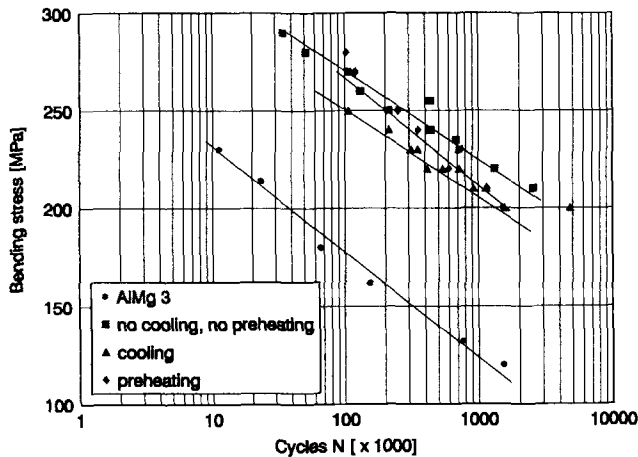


Fig. 10 *S/N* diagram as a function of substrate temperature

measurements were performed in the range of the fatigue limit (10^3 to 10^6 cycles) for each parameter set. The results of those sets in which one parameter was varied were compared. Figure 8 shows the test sample design.

The stress-cycle (*S/N*) diagram of the raw material was compared with that of the sprayed substrate to establish any changes in fatigue properties that arose from the thermal spray coating process. Analysis of the experiments revealed three characteristic *S/N* curves (Fig. 9). Type 1 behavior is exhibited when the *S/N* curve is parallel and translated above that of the uncoated material. A type 2 response shows an *S/N* curve that is parallel and translated under that of the uncoated material. In type 3 behavior, the slope of the curve decreases and the curve intersects that of the uncoated material. For each of the different process parameters, evaluation with respect to the cyclic stress is as follows:

- *Type 1*: The parameter influences the alternating stress resistance positively.
- *Type 2*: The parameter influences the alternating stress resistance negatively.
- *Type 3*: The alternating stress resistance of the raw material is not negatively affected, but higher amplitudes of the stress may not be endured.

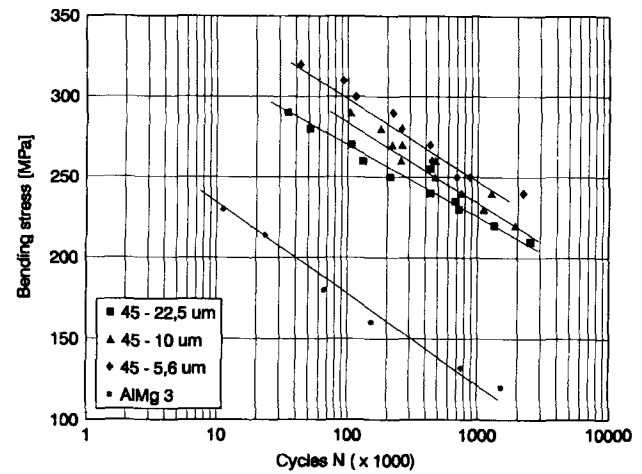


Fig. 11 *S/N* diagram as a function of powder grain-size range

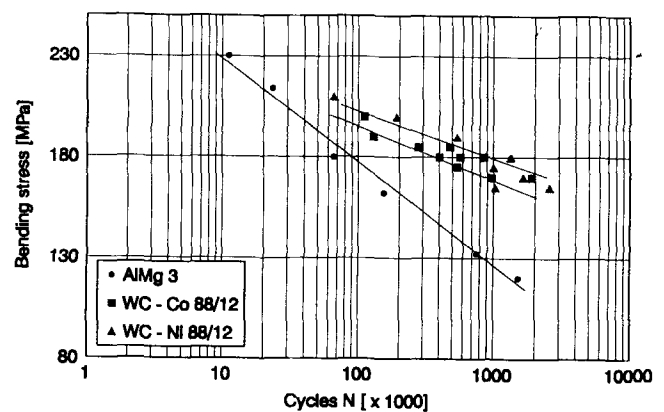


Fig. 12 *S/N* diagram as a function of metal matrix material (same WC concentration)

4. Results

The classification outlined in the preceding section is used in this section to examine the experimental results. Again, it should be mentioned that residual stress depends on the shape of the component; therefore, exact prediction of the lifetime of an engineering component is very complicated.

4.1 Substrate Temperature

During the thermal spray process, the substrate temperature rises until a constant value is reached. When spraying small parts, this value should be controlled by substrate cooling because the maximum temperature is inversely related to the part dimensions. In large parts, the heat disperses and is dissipated over the surface. This effect was the subject of the first series of tests (Fig. 10). The frame used in this study was like that shown in Fig. 6, with a diameter of 250 mm. This arrangement allows control of the substrate temperature. The following test variations were used on the steel and aluminum specimens: cooling

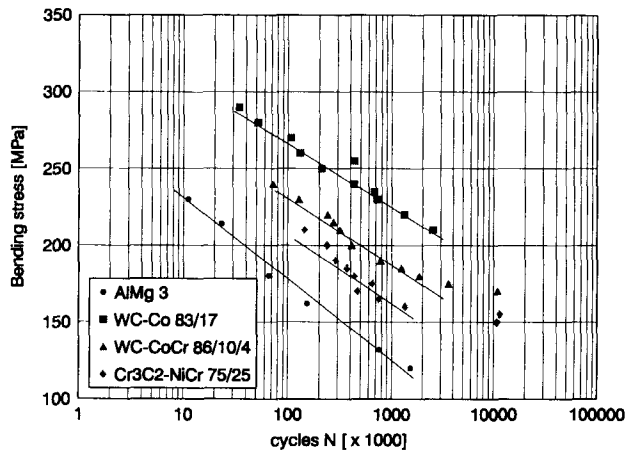


Fig. 13 S/N diagram as a function of coating material

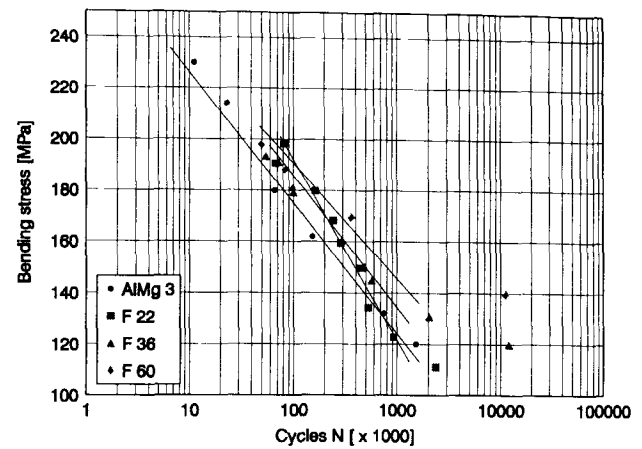


Fig. 14 S/N diagram as a function of grit-blasting material

Table 3 Grit-blasting parameters

Type	Grain size, μm	Roughness (R_a), μm
F 22	600-1180	10.5
F 36	355-710	7.4
F 60	180-355	4.0

of the substrate by airflow, preheating of the substrate, and spraying without cooling or preheating.

Aluminum test samples exhibited type 1 S/N diagrams, and steel samples resulted in type 3 S/N diagrams. The reason for this effect is the different Young's moduli of steel and aluminum. On both materials, the value of fatigue resistance increases with increasing substrate temperature during spraying. The residual stress distribution caused by preheating increases the fatigue limit.

4.2 Powder Grain Size

A range of powder grain sizes is often used in HVOF processes. An agglomerated sintered WC-17Co powder with three different grain size ranges (45 to 22.5 μm , 45 to 10 μm , and 45 to 5.6 μm) was used in this series of experiments. These are representative of a typical commercial product.

In all three classes, the applied coating showed the same microhardness ($HV_{0.3} = 1050$) and a porosity volume fraction of less than 1%. The resulting S/N diagram was type 1 in all three cases (Fig. 11). The experiment with the lowest grain-size limit (5.6 μm) exhibited the best results.

4.2 Composition

A higher loading with 88% WC yielded an S/N diagram of type 3 (Fig. 12). When nickel is used instead of cobalt, fatigue resistance decreases. Tests using $\text{Cr}_3\text{C}_2\text{-}25\text{NiCr}$ and WC-10Co-4Cr powders resulted in an S/N diagram of type 1, close to the result for WC-17Co powder (Fig. 13).

4.4 Grit Blasting

Grit blasting can be used to induce compressive residual stress into surfaces. This subject was tested on aluminum substrates in a fatigue bending test with Al_2O_3 blasting materials. The different blasting parameters are given in Table 3. The air-flow pressure was 0.25 MPa, the standoff distance between torch and substrate 100 mm, and the torch angle 60°.

Type 1 S/N diagrams (Fig. 14) resulted when using F 36 and F 60 grit-blasting materials. A larger increase in endurance limit was reached using F 60 for blasting. A high surface roughness value induced notches when blasting with F 22. A lower endurance limit was reached in the S/N diagram because of the surface roughness caused by grit blasting. These effects are relevant only for noncoated surfaces. The endurance limit was not influenced by polishing or brushing of the coated surface (compared to the as-sprayed surface) or by variations in turning speed and torch traverse speed by $\pm 20\%$ from the baseline conditions.

5. Conclusions

Carbide coatings produced by the HVOF process with porosity levels of less than 1% behave like a homogeneous material, with a fixed ductility. Their high E value allows a higher stiffness for aluminum constructions.

Steel or aluminum substrates with HVOF coatings exhibit no negative change in endurance limit. Exact calculation of the endurance limit or maximum tensile strength requires that the residual stress condition be known. Machine parts with a carbide HVOF coating can be safely designed by ensuring that the maximum stress not exceed the endurance limit of the substrate material.

Acknowledgments

The author would like to thank Deloro Stellite GmbH, Koblenz; Metco, Hattersheim; Plasma-Technik AG CH-Wohlen; UTP, Bad Krozingen; and Torsten O.D. Lüddecke.

References

1. T.M. Weber and V. Messerschmidt, Hochgeschwindigkeitsflammspritzen in der Praxis, *Schweissen Schneiden*, Vol 45 (No. 2), 1993, p 95-98 (in German)
2. W. Bertram and M. Schemmer, Haftfestigkeit von Metallschichten auf Stählen bei statischer und wechselnder Beanspruchung, *Z. Werkstofftechnik*, Vol 16, 1985, p 1-12 (in German)
3. H.-D. Steffens and H. Bastert, Dauerschwinguntersuchungen an metallgespritzten Stahlproben, *Härt. Tech. Mitt.*, Vol 22 (No. 3), 1967, p 221-233 (in German)
4. R. Knight and R.W. Smith, Residual Stress in Thermally Sprayed Coatings, *Proc. Natl. Thermal Spray Conf.* (Anaheim, CA), 1993. p 607-612
5. O. Buxbaum, *Betriebsfestigkeit Sichere und wirtschaftliche Bemessung schwingbruchgefährdeter Bauteile*, Verlag Stahleisen mbH, Düsseldorf, Germany, 1986, p 129-130 (in German)